DOI: https://doi.org/ 10.15276/aait.02.2019.5
UDC 621.923.1:621.833

COMPARISON OF MEASURED SURFACE LAYER QUALITY PARAMETERS WITH SIMULATED RESULTS

Natalia V. Lishchenko[1)]
ORCID: 0000-0002-4110-1321, odeslnv@gmail.com
Vasily P. Larshin[2)]
ORCID: 0000-0001-7536-3859, vasilylarshin@gmail.com
[1)] Odessa National Academy of Food Technologies, 112, Kanatnaya, St. Odesa, 65039, Ukraine
[2)] Odessa National Polytechnic University, 1, Shevchenko Avenue. Odesa, 65044, Ukraine

ABSTRACT

The grinding temperature is one of the factors limiting the throughput performance of the profile gear grinding operation. There are two main methods for determining the grinding temperature: an analytical method with the aid of analytical models and a simulation one based on both the analytical and geometrical models. In the paper, at the first stage the profile gear grinding temperature field is investigated with the aid of finite element method (FEM) simulation as an example of information technology which helps to predict the surface layer quality physical parameters. The results obtained are compared with similar calculations for the analytical models and the tooth surface area is found to determine the temperature according with the analytical models. At the second stage, a series of experimental studies on the CNC machine Höfler Rapid 1250 is carried out on a real gear by means of a successive increase in the depth of profile gear grinding. From the gear machined the special samples were cut out on the electro-erosive machine mod. MV 2400S ADVANCE Type 2 (MITSUBISHI ELECTRIC Company) for additional investigation of these samples. The teeth surface layer quality experimental study and the structural-phase state of the surface layer metallographic analysis have been performed using modern measuring equipment and instruments, e.g. microscope Altami MET-5. It is established that, in other equal conditions, the highest grinding temperature occurs in the upper part of the tooth which is grinding. It is identified areas of the tooth profile, on which the grinding temperature can be calculated by the famous analytical dependencies. It is established that as the parameters characterizing the grinding intensity and the volume of material removal per unit of the grinding wheel width increase, the grinding burn arises and its thickness increases. The regularity of the change in the thickness of the burn along the height of the tooth is established, which makes it possible to evaluate the reliability of the corresponding theoretical studies.

Keywords: Profile Gear Grinding; Grinding Burn; Surface Layer Quality; Grinding Temperature; FEM Simulation

***For citation*: Lishchenko N. V., Larshin V. P.Comparison of Measured Surface Layer Quality Parameters with Simulated Results. *Applied Aspects of Information Technology.* 2019; Vol. 2 No. 4 304–316. DOI: https://doi.org/ 10.15276/aait.02.2019.5**

INTRODUCTION

It was established in [1, 2] that one of the factors limiting profile grinding productivity is the temperature in the cutting zone. Grinding temperature excess leads to grinding burns and cracks. The relationship between the gear grinding productivity and its limiting factors was considered when developing a methodology for studying the technological system of gear grinding [3]. Grinding burns arise at some point in time as the grinding intensity increases and the cutting power of the grinding wheel changes in its blunting, greasing, etc. Most researchers [4, 5], [6, 7], [8, 9], [10, 11], [12] consider that the temperature factor is responsible for the occurrence of grinding burns, and connect the appearance of the burns with the so-called critical grinding temperature which is not constant and depends on the duration of high temperature and its rate of change [5].

At this time, the detection and study of burns in grinding is one of the problematic issues in engineering technology in connection with the uncertainty of the conditions of its occurrence. Existing methods for determining the presence and magnitude of burns are divided into two groups: destructive (cutting micro slices from the gear which have been ground) and non-destructive (acid etching, current strain control, the Barkhausen noises method, etc.) [13,14], [15,16].

Each of these methods has its advantages and disadvantages. For example, after the use of destructive methods, one of the parts of the batch is to be disposed of. After acid etching of teeth, the contact strength of the gears decreases up to 20 %. From the non-destructive methods, the Barkhausen noises method was the most widely used, according to which the detection of burns is performed on the basis of control of changes in the electromagnetic properties of the gear material [6], [17]. All these and related issues are considered in the relevant literature [6], [17,18], [19,20], [21,22], [23,24], [25].

Typically, grinding burns are detected by comparing the modified and initial structures of the material in the studied region. Therefore, the methods of preliminary planning of relevant experiments are commonly used [6]. Among the production methods include the method of acid etching and the method of visual control, the modification of which allows increasing the reliability of the detection of grinding burns.

ISSN 2617-4316 (Print)
ISSN 2663-7723 (Online)

Analysis of the literature shows that most studies refer to the flat and round grinding operations. The specificity of the profile grinding is reflected in a much smaller number of literary sources. For example, in [25], it is shown that when profile grinder working on the radial in feed method, the burns appears in the upper part of the tooth. However, in the literature there is no data on the study of the topography of grinding burns along the height of the tooth. There is no information on ensuring defect-free grinding under uncertainty conditions when burn appearance and their change along the tooth height take place.

There are two approaches to determining the grinding temperature: the phenomenological - on the basis of the Fourier differential equation of the thermal conductivity (analytical method of temperature determination) [8], [11,12], [26,27], [28,29], [30,31], [32,33], [34,35] and temperature field simulation - on the basis of computer simulation by the method of finite elements (FEM Simulation) [36,37], [38,39], [40,41].

Analytical solutions require the assumptions and do not allow considering factors such as the variable heat flux density of the thermal flow along the height of the tooth, the geometric shape (dimensions, curvature) of the involutes gear surface, etc. The simulation method is used to determine the temperature field in profile grinding, taking into account cooling, the movement of the contact area, the variable heat flux density along the height of the tooth, the geometric shape of the object, to evaluate the selected analytical mathematical dependence, to determine the range of its action, based on the permissible error of temperature determination.

Information 2D and 3D models

The geometrical model of a gear tooth is set in the AutoCAD software and imported into the COMSOL Multiphysics (Fig. 1a). The tooth involute profile contact zone is divided into 99 sections of equal area. The heat flux density is given on each of these sections, which at each point of the involute tooth profile is determined by the formula [42]

The geometrical model of a gear tooth is set in the AutoCAD software and imported into the COMSOL Multiphysics (Fig. 1a). The tooth involute profile contact zone is divided into 99 sections of equal area. The heat flux density is given on each of these sections, which at each point of the involute tooth profile is determined by the formula [42]

$$q(r_x) = e_c \psi \frac{dQ_w}{dS_c} = \frac{P}{V_f S_{cc}} \psi \frac{V_f t_n(r_x)}{\sqrt{D t_v(r_x)}}, \qquad (1)$$

where: e_c is a grinding specific energy of, J / m^3; ψ is a grinding heat partition ratio; $Q_w$is a material removal rate, m^3/s; S_c is a contact area, m^2; P is a grinding power, W; V_f is an axial feed, m/s; S_{cc} is a cross-sectional area of the section, m^2; t_v is a grinding vertical depth, m; t_n is a grinding normal depth, m; r_x is a current radius-vector, m; D is a instant grinding wheel diameter, m..

The initial data for determining $q(r_x)$ are given in the Table 1.

To determine the instantaneous normal depth of grinding, one can use either the techniques of differential geometry [43] or the known equation of connection between vertical and normal grinding depths [8]

$$t_n = t_v \cos\gamma \qquad (2)$$

where: γ is the angle between the normal to the involute and the axis of symmetry of the gap gear.

3D Geometric model

The geometric model of the gear tooth (Fig. 1b) was created in the AutoCAD program and imported into the COMSOL Multiphysics. The contact area (Fig. 2) of the grinding wheel and the gear (moving thermal source) is the *A-B-C-D* section, which is common between the grinding wheel and the gear. Involute profile of the tooth consists of 99 sections. Each of them has a heat flux density defined by the formula (1) at each point of the involute profile.

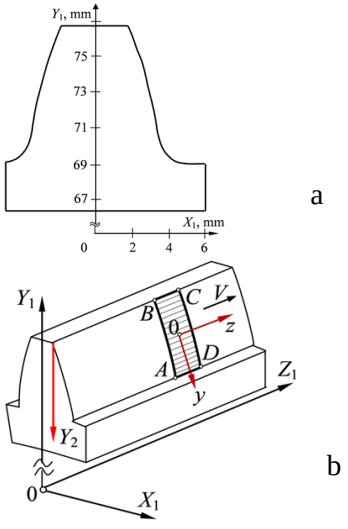

Fig. 1. **Geometric models: 2D (a) and 3D (b)**
***Source*: compiled by the author**

The contact area has the height $(r_a - r_b)$ and width $2h$ and $h = \sqrt{D \cdot t_v} / 2 = \sqrt{400 \cdot 0,074} / 2$ $=2,72 \cdot 10^{-3}$ m or $2h = 5,44 \cdot 10^3$ м, або 5,44 mm. The time of the thermal source action is determined by the formula

$$\tau_H = \frac{2h}{V_f} = \frac{\sqrt{D \cdot t_v}}{V_f} \quad (3)$$

where: h is the half-width of the contact area in the direction of the velocity vector of the part, mm.

In this case $\tau_H = \frac{\sqrt{D \cdot t_v}}{V_f} = \frac{\sqrt{400 \cdot 0,074}}{116,67} = 0,0466$ c, i.e., τ_H = 46,6 ms.

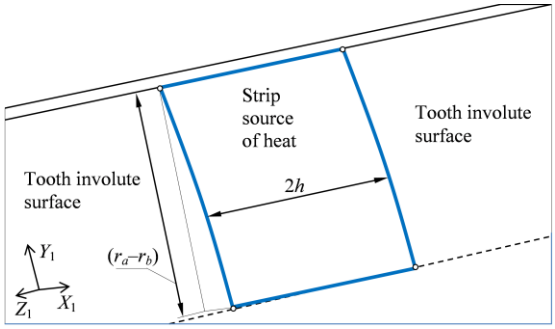

Fig. 2. **Gear tooth with strip heat source**
***Source*: compiled by the author**

Table 1. **Different parameters and conditions in grinding**

Parameters	Data
Workpiece material	20X2H4A (analog to19CrNi8 Germany, 3120 USA)
Specific energy (e_c)	54 J/mm^3
Grinding heat partition ratio to the workpiece (ψ)	0,8
Initial wheel diameter (D)	400 mm
Vertical grinding depth (t_v)	0,074 mm
Axial feed (moving heat source velocity V_f)	116,67 mm/s (7 m/min)
Thermal diffusivity (a)	5,683·10^{-6} m^2/s
Thermal conductivity of the workpiece (λ)	24 W/(m·°C)
Density of the workpiece (ρ)	7850 kg/m^3
Heat capacity (c)	538 J/(kg·°C)
Number of teeth (z)	40
Normal module (m)	3,75 mm
Diameter of the pitch circle (d)	150 mm
Diameter of the outside circle (d_a)	153,75 mm
Diameter of the base circle (d_b)	140,954 mm
Diameter of the root circle (d_f)	139,875 mm
Face width (B)	24 mm
Pressure angle of involute (α)	20°
Helix angle (β)	0

***Source*: compiled by the author**

Gear grinding temperature simulation results

Simulation of the temperature field in the COMSOL Multiphysics is performed and–the following conclusions are formulated.

1) 2D and 3D simulation of the temperature field allowed determining the surface temperature under 2D simulation of the temperature field with an error of not more than 5 % compared with the results of 3D simulation under other equal conditions, when the heating time τ_H under 2D simulation is equal to the heating time from the unmoving source of heat $\tau_H = 2h / V_f$. Moreover, at $V_f \geq$ 5 m/min the mentioned error does not exceed 1 %.

2) It is shown that in the axial feed range 1 $\leq V_f \leq$ 12 m / min the difference between the results of temperature determination under 2D and 3D simulation is 0,71 … 4,03 %. This confirms the possibility of replacing a moving thermal source by the stationary one, whose thermal source action time depends on the moving source velocity V_f and is equal to $\tau_H = 2h / V_f$. For example, a minimum error of 0,71 % when determining the temperature for 2D (Fig. 3) and 3D models (Fig. 4b) is obtained at V_f = 7 m/min.

3) With an increase in axial feed V_f from 1 m/min to 12 m/min, the maximum temperature increases for a moving heat source from 248 °C to 923 °C, while for the unmoving one – from 258 °C to 936 °C. This correspondence confirms the identity of the results of determining the surface maximum temperature for these solutions under 2D and 3D simulation. In other equal conditions, the maximum temperature for a moving source (248 °C … 923 °C) is less than for the unmoving one (258 °C… 936 °C) throughout the range of axial feed interval of 1 $\leq V_f \leq$ 12 m/min.

It is found that the maximum values of temperature (Fig. 5a) and the heat flux density (Fig. 5b) are located at the upper part of the involute profile and do not match the height of the tooth, and the maximum temperature is below the maximum of the heat flux density located on the tooth tip.

It should be noted that the 2D geometric model in simulation corresponds to a one-dimensional analytic solution with a variable heat flux density.

ISSN 2617-4316 (Print)
ISSN 2663-7723 (Online)

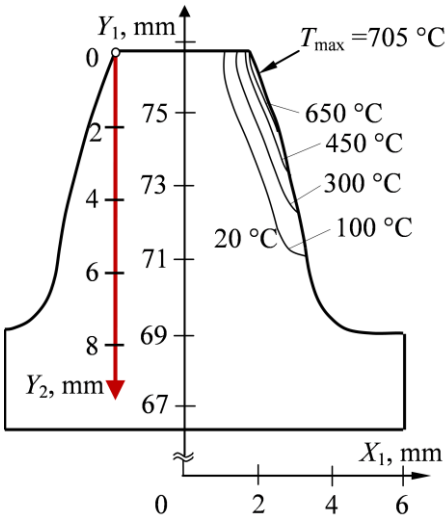

Fig. 3. **Temperature field isotherms for 2D model**
***Source*: compiled by the author**

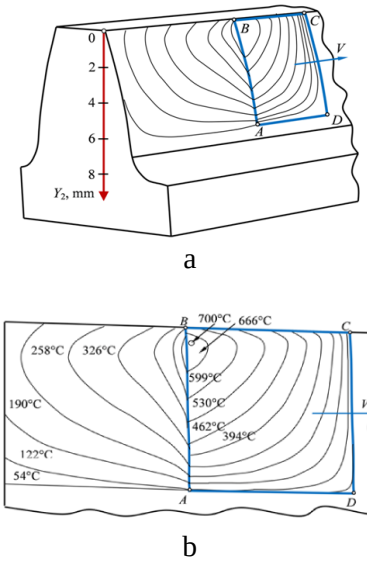

Fig. 4. **Steady temperature field isotherms for 3D model (a) and his fragment (b) for τ=103,5 ms**
***Source*: compiled by the author**

To determine the profile gear grinding temperature using the solution of a one-dimensional differential heat equation, the following concept was adopted. The indicated (one-dimensional) solution can be used to determine the temperature in the center of several areas of the involute profile surface of the tooth (gap) located at the height of the tooth, for example, in the upper, middle and lower areas of the involute profile. The number of these areas should be both minimal and sufficient. The condition of parallelism of the heat flux density vectors occurs when there is a "sufficient" surface area with a variable heat flux density, which can be characterized by its average value (mean value). It is obviously, this condition is most fulfilled at the point of the contact area, which is equidistant from the edges of this zone.

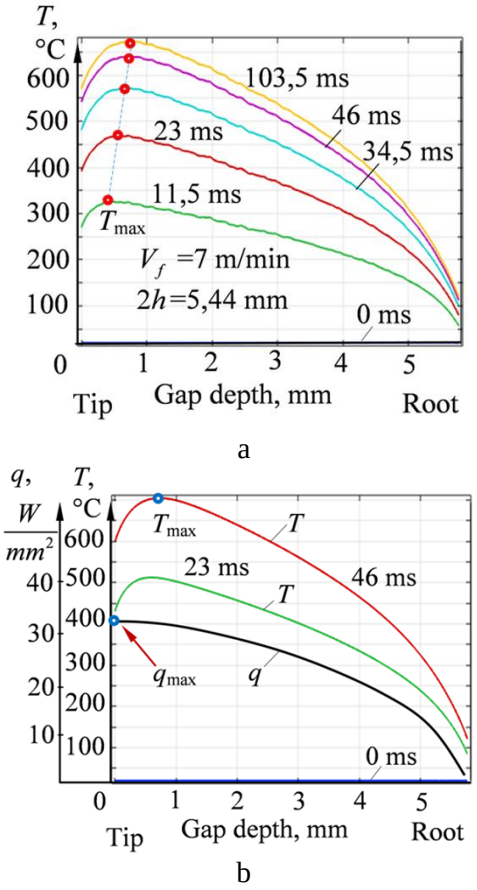

Fig. 5. **The surface temperature *T* of the involute profile under variable heat flux density *q* for a moving heat source of width 2*h* on the its back edge (a) and for the unmoving one (b)**
***Source*: compiled by the author**

The equation describing the one-dimensional temperature field $T_н(x,\tau)$ over the heating time interval $0 \le \tau \le \tau_H$ has the form [44; 45]

$$T_H(x,\tau) = \frac{2 \cdot q\sqrt{a \cdot \tau}}{\lambda} \cdot \text{ierfc}\frac{x}{2\sqrt{a \cdot \tau}}, \qquad (4)$$

where τ is the duration of the unmoving heat source action and $0 \le \tau \le \tau_H$, s; $\text{ierfc}\, u$ is the designation of a special function which is [46]:

$$\text{ierfc}\, u = \frac{1}{\sqrt{\pi}} \exp\left(-u^2\right) - u\, \text{erfc}\, u \quad \text{i}$$

$$\text{erfc}\, u = \frac{2}{\sqrt{\pi}} \int_u^{\infty} \exp\left(-u^2\right) du\,.$$

Therefore, the next stage of the temperature field simulation is determining the number of areas in which the profile grinding temperature can be determined by solving the one-dimensional differential equation of heat conduction by the formula (4).

For a comparative analysis, a number of the variants of imaging contact zone by areas on the involute profile of the tooth for a one-dimensional solution are predetermined: 1 area (Fig. 6a), 2 areas (Fig. 6b), 3 areas (Fig. 6c) and 6 areas (Fig. 6g). The heat flux density is given equal to its averaged value which are found through relevant instant values of $\overline{q}_{i,j}$, i.e. in this case $1 \le i \le 6$, $14 \le j \le 99$.

For example (Fig. 6): $\overline{q}_{1,99}$ = 21,45 W/mm²; $\overline{q}_{1,49}$ = 26,93 W/mm²; $\overline{q}_{2,50}$ = 15,85 W/mm²; $\overline{q}_{1,33}$ = 28,36 W/mm²; $\overline{q}_{2,33}$ = 22,51 W/mm²; $\overline{q}_{3,33}$ = 13,47 W/mm²; $\overline{q}_{1,17}$ = 29,61 W/mm²; $\overline{q}_{2,17}$ = 26,96 W/mm²; $\overline{q}_{3,17}$ = 23,96 W/mm²; $\overline{q}_{4,17}$ = 20,43 W/mm²; $\overline{q}_{5,17}$ = 15,97 W/mm²; $\overline{q}_{6,14}$ = 9,70 W/mm².

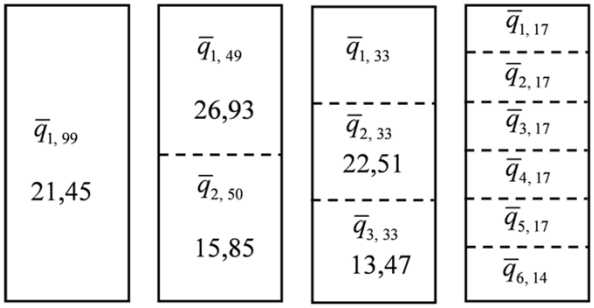

Fig. 6. **Contact zone consisting of 1 area (a), 2 areas (b), 3 areas (c) and 6 areas (g) for 2D simulation model**

***Source*: compiled by the author**

The cause-effect relationships in the direction from the heat flux density $\overline{q}_{i,j}$ (cause) to the temperature (consequence) are explained graphically in Fig. 7.

It can be seen that the result of the step-heat flux during the two time intervals (23 ms and 46 ms) is three surface temperatures:

– two continuous temperatures curves obtained by the method of 2D simulation at τ_H = 23 ms (green) and τ_H = 46 ms (red);

– the temperature obtained by the calculation of a one-dimensional solution of the differential equation of heat conduction (4) at τ_H = 46 ms (black dotted line).

It can also be seen that at τ_H = 46 ms, the maximum temperature under the stepped heat flux (Cause on Fig. 8) with 2D simulation (first comparable version) and maximum temperature by analytical one-dimensional solution (second comparable version) are $T_{MAX} = T_1'$ =699 °C and 686,52 °C, respectively. That is, the difference is 1,79 % (no more than 2 %).

Let's compare the obtained maximum temperatures (699 °C … 686,52 °C) with the maximum temperature from the influence of the variable heat flux density on the coordinate Y_2 (Fig. 5b). To do this, the conversion of the dependence $q(r_x)$ to the dependence $q(Y_2)$ has been made. This case (Fig. 8) under other equal conditions is more close to reality. It can be seen that the maximum temperature in this case is 705 °C, it differs from the result of calculating according to the one-dimensional solution (686,52 °C) of the differential heat conduction equation by 2,6 %. Thus, the considered method of using a one-dimensional solution is the basis which allows this solution use to determine the profile gear grinding temperature. The T_1, T_2, T_3 temperatures obtained (Fig. 8) are in the middle of the corresponding three areas. The temperatures for one, two, and six areas (Table 2) can be determined similarly.

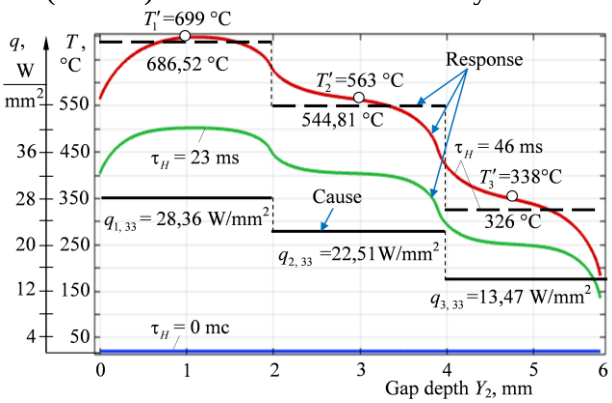

Fig. 7. **The average heat flux density and temperature responded on the gap depth for the three areas; 686,5 °C; 544,8 °C; 326,0 °C are the temperatures found by one-dimensional analytical solution (4) at heating time 0, 23, and 46 ms**

***Source*: compiled by the author**

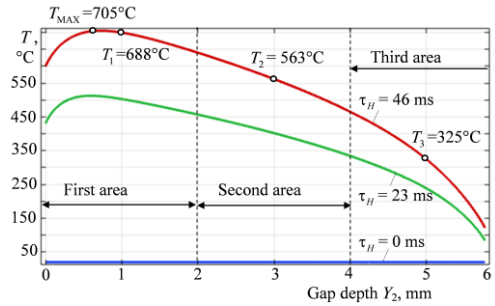

Fig. 8. **The temperature on the gap depth under the variable heat flux density $q(r_x)$ for 2D simulation for three areas at heating time: 0, 23, and 46 ms**

***Source*: compiled by the author**

ISSN 2617-4316 (Print)
ISSN 2663-7723 (Online)

Table 2. **Maximum surface temperature determination results on the basis of the temperature field 2D simulation at τ_H = 46 ms**

Areas numbers							
1		2		3		6	
T_1, °C	562,5	T_1, °C	675	T_1, °C	688	T_1, °C	700
		T_2, °C	400	T_2, °C	563	T_2, °C	675
				T_3, °C	325	T_3, °C	600
						T_4, °C	520
						T_5, °C	400
						T_6, °C	225
Note: the maximum temperature in the contact zone in 3D simulation T_{MAX} = 705 ° C							

***Source*: compiled by the author**

Corresponding data for different number of areas (1, 2, 3 and 6) are presented in Table 2. When the profile is divided into 3 areas with an average heat flux density in each of them, the minimum error in the definition of T_{MAX} is 0,84 % (Table 2) compared with the maximum temperature found at the instant heat flux density: ((705-699)/705) x100 %= 0,84 %.

Thus, the contact zone (Fig. 9a) can be represented by the spot consisting of three areas (Fig. 9b) with the heat flux density averaged over these areas.

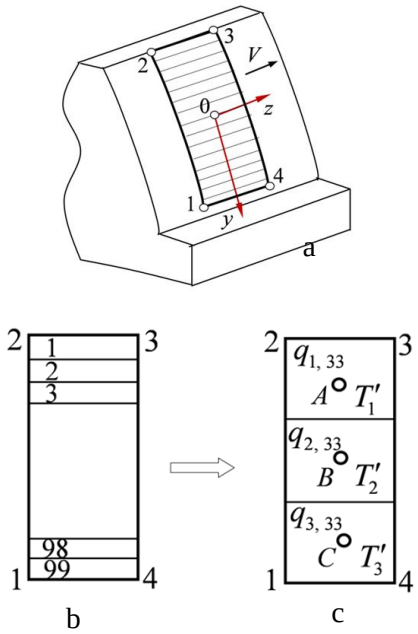

Fig. 9. **Stages of the transformation of moving rectangular source (a) into unmoving one, which consists of 99 (b) and 3 (c) areas**
***Source*: compiled by the author**

SURFACE LAYER QUALITY PHYSICAL PARAMETERS STUDY

The study of the teeth surface layer quality after the profile grinding is one of the most labor-intensive works as it involves extracting fragments and samples to study them. It is known the grinding burns arise from the influence of the temperature factor in the cutting zone, but the possibility of their occurrence depends on a large number of parameters. The literary analysis of the state of the question showed that most researchers plan appropriate experiments by successively changing the value of any parameter that has an effect on the grinding temperature. In this regard, for the experimental determination of defect-free depth of grinding, a special experiment was conducted at a constant axial feed V_f = 5000 mm/min with the following discrete grinding depths (t_n): 0.035 mm (the gap between 28 and 29 teeth); 0.050 mm (the gap between 29 and 30 teeth); 0.075 mm (the gap between 30 and 31 teeth); 0.090 mm (the gap between 31 and 1 teeth) (Fig. 10), that is, we have the following data:

t_n, мм…….0,03 0,050 0,075 0,090,

The gap place…28-29 29-30 30-31 31-1.

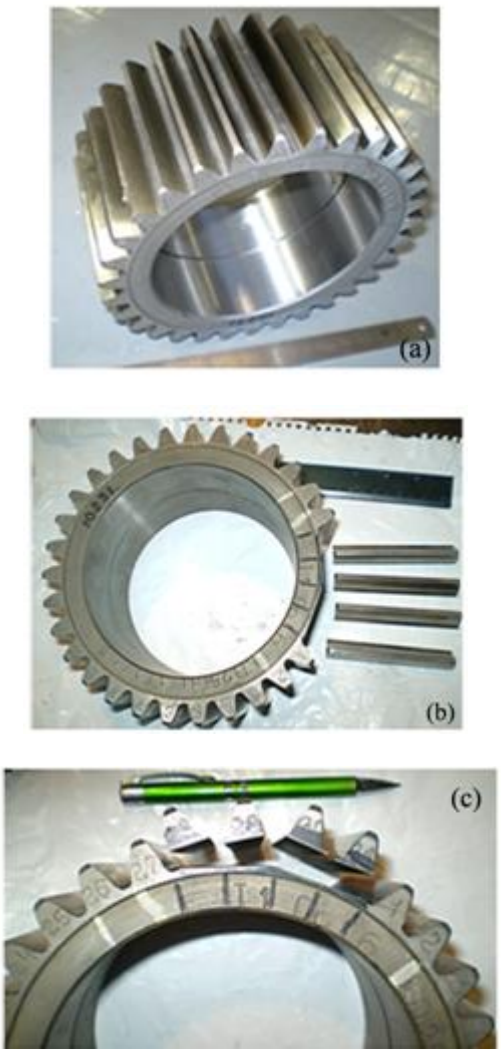

Fig. 10. **Grounded gear before (a) and after (b, c) cutting off the four teeth**
***Source*: compiled by the author**

The cutting off these four teeth was made on an electro-erosion machine MV 2400S ADVANCE Type 2 (MITSUBISHI ELECTRIC). After cutting off the teeth and their fragments, the surfaces studying were prepared on a flat-grinding machine with the help of simple equipment (Fig. 11).

Studies of the samples microstructure 28-31 were performed on micro slips (Fig. 12) after etching their surface by the solution of 2-3 % nitric acid in alcohol. The micro-hardness of the surface layer depth was determined using the PMT-3 instrument (Fig. 13a), the metallographic studies of the micro-slips were performed on the Altami MET-5 microscope. (Fig. 13b).

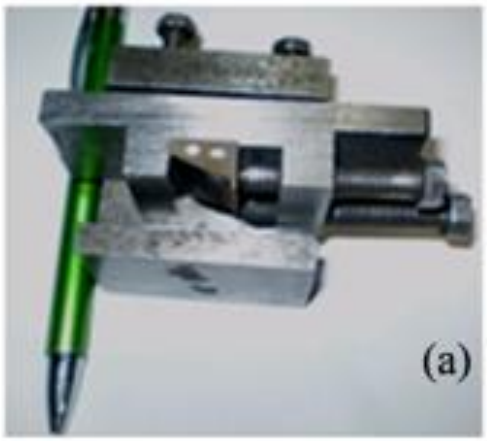

Fig. 11. **Samples prepared from fragment teeth when the sample is clamped in the fixture (a) and installed onto the machine table (b)**
***Source*: compiled by the author**

On the surface of samples 28 (Fig. 14) and 29 (Fig. 15), a cemented layer is observed and no burns are detected. Structural-phase transformations are observed on the surface of samples 30 (Fig. 16) and 31 (Fig. 17), which are also confirmed by the change in the microhardness of the depth of the surface layer (Fig. 18).

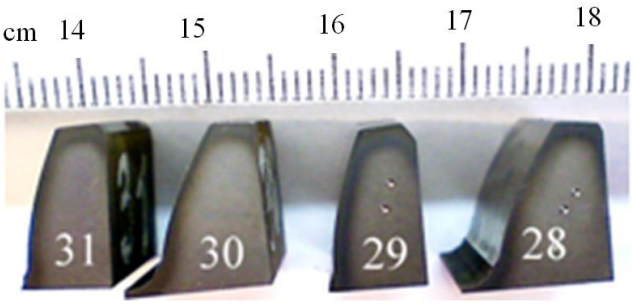

Fig. 12. **The samples of teeth (28–31) and their faces for study**
***Source*: compiled by the author**

Fig. 13. **Hardness measurements both on PMT-3 instrument (a) and microscope Altami MET-5 (b)**
***Source*: compiled by the author**

Measurements of micro hardness were performed in the upper, middle and lower parts of the tooth (Fig. 18).

ISSN 2617-4316 (Print)
ISSN 2663-7723 (Online)

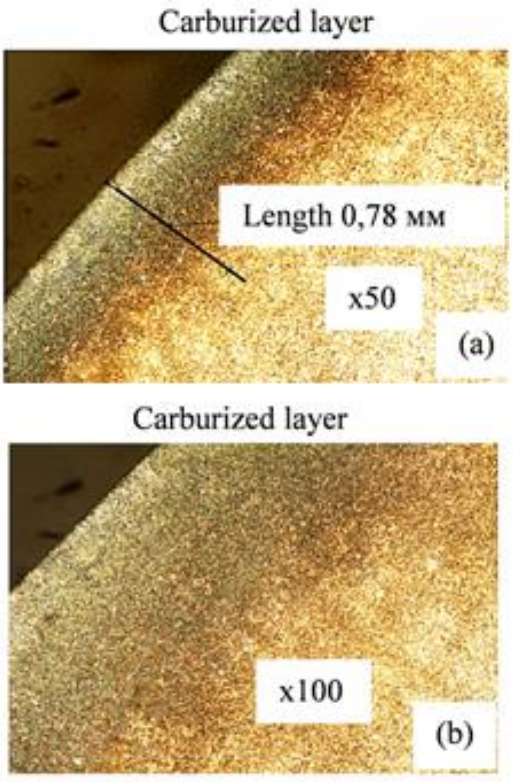

Fig. 14. **Sample surface microstructure of the tooth 28 with an increase of x50 (a) and x100 (b)**
***Source*: compiled by the author**

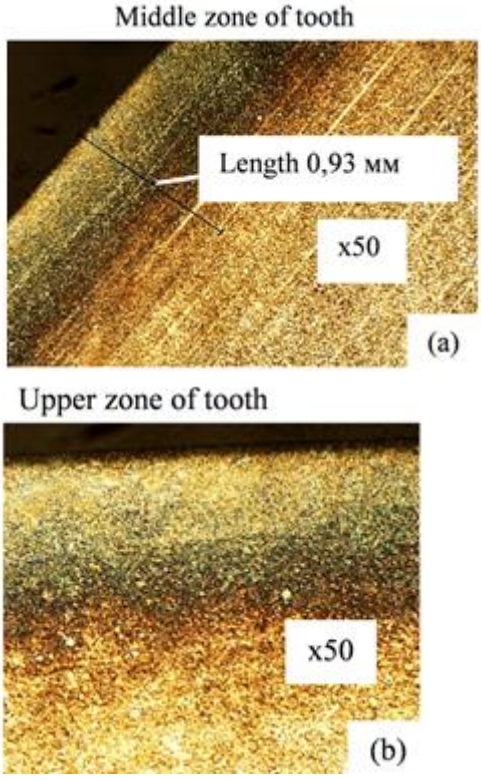

Fig. 15. **Sample surface microstructure of the tooth 29 in the middle (a) and upper (b) zones**
***Source*: compiled by the author**

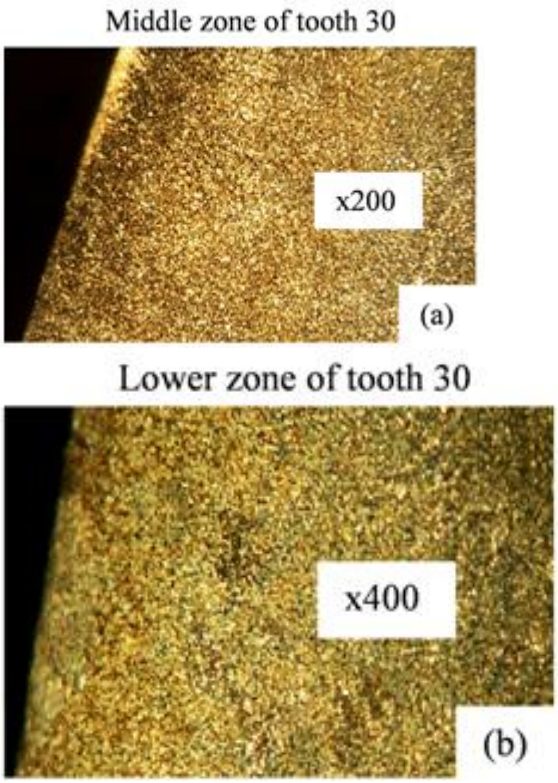

Fig. 16. **Sample surface microstructure of the tooth 30 in the middle (a) and lower (b) zones**
***Source*: compiled by the author**

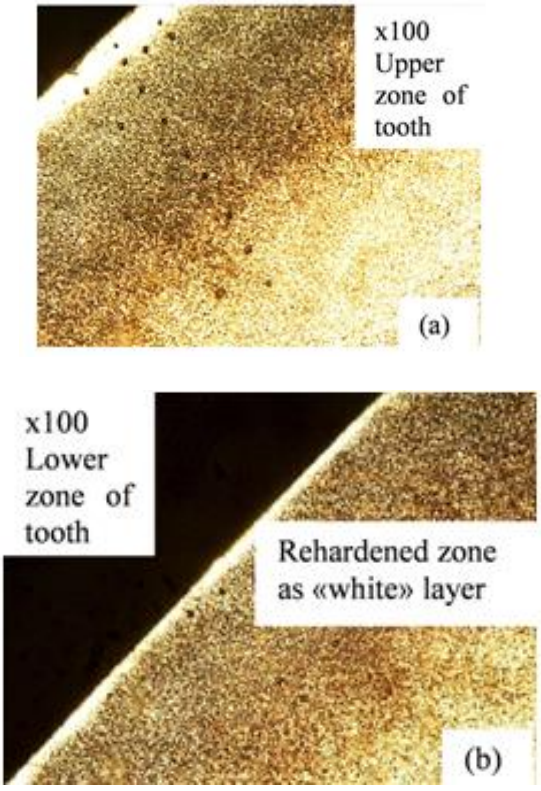

Fig. 17. **Sample surface microstructure of the tooth 31 in the tip (a) and root (b) section**
***Source*: compiled by the author**

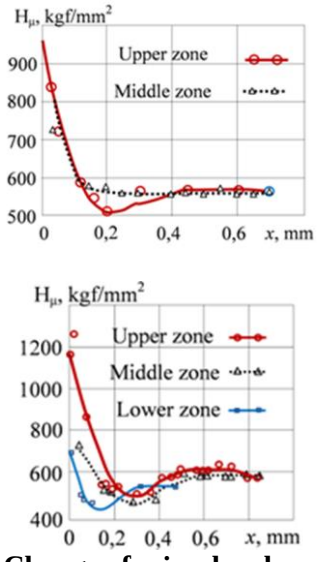

Fig. 18. **Change of microhardness on the depth of the surface layer of teeth 30 (a) and 31 (b) on the tooth different sections at its height (tip, middle and root)**

***Source*: compiled by the author**

As the normal cutting depth t_n increases from 0,035 to 0,09 mm with a constant axial feed V_f = 5000 mm/min, the grinding burns arises and increases in the tooth surface layer (see the curves $h_{w.l.}$ and $h_{d.l.}$ in Fig. 19). At the same time the Q'_w and V'_w parameters is increasing.

The points A1 and B1 correspond to the operating characteristics of the conventional 25AF46L6V grinding wheel. In turn, the points A2 and B2 correspond to high-porous wheel, for example, the wheel 3SG46Hs12Vs. As the grinding depth increases, the burn defective layer, consisting of the re-hardened "white" layer and tempered layer (not shown in Fig. 10).

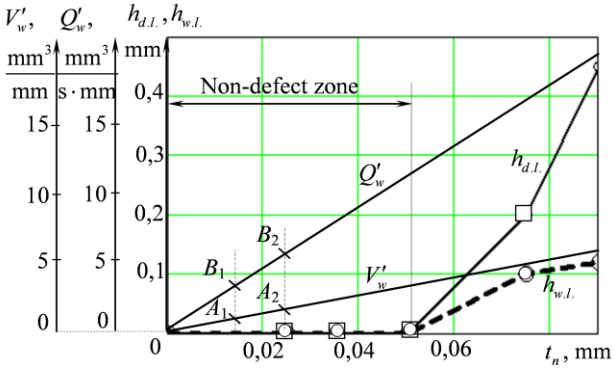

Fig. 19. **Influence of the grinding normal depth on the thickness of the emerging "white" layer $h_{w.l.}$, the total depth of the defective layer $h_{d.l.}$, as well as the parameters Q'_w and V'_w**

***Source*: compiled by the author**

Thus, improving the operating characteristics of the grinding wheel (the combination of parameters Q'_w, and V'_w) allows you to increase the grinding depth without the defect zone (Fig. 19). The tendency to change the depth of the defective layer by the height of the profile is such that its largest thickness is at the top of the profile height at a distance from the edge of the contact area (Fig. 19). It is known that at the edge of the contact zone, the grinding temperature is twice lower than in the middle of this zone, even with the same density of heat flux density [26]. This experimentally discovered fact confirms the expediency of determining the grinding temperature for one-dimensional solutions of the differential heat equation, in which the density of the heat flux is constant within the contact zone and is equal to its average value within the specified zone. Continuous increase of parameters $Q'_w(t_n)$ and $V'_w(t_n)$ correspond to "threshold dependencies" $h_{d.l.}(t_n)$ and $h_{w.l.}(t_n)$ with threshold level t_n=0.05 mm (Fig. 19). This at the level of the dividing circle corresponds to the vertical grinding depth $t_v = \frac{t_n}{\sin\alpha}$ = 0,146 mm, where α – the profile angle).

The performed experimental studies confirm the position of the points on the involute profile (Fig. 20), which determine the grinding temperature for a one-dimensional solution of the differential heat equation.

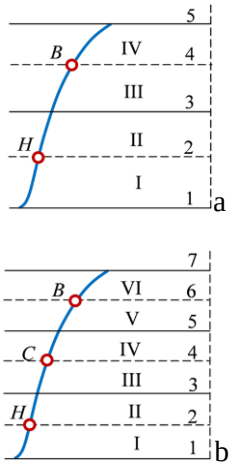

Fig. 20. **The points *H* and *B* (a) and also the points *H*, *C* and *B* (b) on the involute profile for the grinding temperature theoretical determination**

***Source*: compiled by the author**

The position of these points (Fig. 20) determines the mean value of the grinding temperature, which reduces the influence of the edge of the contact area, where a large temperature gradient, which

ISSN 2617-4316 (Print)
ISSN 2663-7723 (Online)

almost twice decreases the temperature at the edge of the zone, takes place.

CONCLUSIONS AND PROSPECTS FOR FURTHER RESEARCH

1. The burn defective layer in the profiled grinding depends on a large number of factors and may appear at a certain critical temperature in the cutting zone which is not a constant value, and depends on the individual actual grinding conditions.

2. In other equal conditions, the defective layer appears when any grinding factor increases, for example, the grinding depth factor. To account for the uncertainty of the conditions of occurrence and increase in the thickness of the defective layer, defect-free grinding should be carried out with some margin (tolerance) on the depth of grinding which takes into account the specified uncertainty (temperature gradient in time, time of acting the critical temperature, etc.).

3. As the grinding stock remains lower, the tolerance zone at the depth of the defect-free grinding must be increased, for example by reducing the grinding depth. In this sense, it is prudent to consider a new approach to the condition of the grinding stock distribution in grinding stages and strokes, according to which the grinding depth, as the reduction of the remaining grinding stock to be removed, is chosen not from the condition of decreasing the defective layer size within the remaining grinding stock, but from the condition of reduction of probability of the defective layer formation. In this case, at each moment of grinding time there will be some stock of allowance within which a defective layer may form and will be removed later with this remaining allowance.

REFERENCES

1. Larshin, V. & Lishchenko, N. “Gear Grinding System Adapting to Higher CNC Grinder Throughput”. *MATEC Web of Conferences.* 2018. Vol. 226 (04033). DOI: https://doi.org/10.1051/matecconf /201822 604033.

2. Larshin, V. & Lishchenko, N. “Adaptive Profile Gear Grinding Boosts Productivity of this Operation on the CNC Machine Tools”. *In:1st International Conference on Design, Simulation and Manufacturing,* DSMIE 2018. Sumy. Ukraine. *Lecture Notes in Mechanical Engineering. Publ. Springer*. Cham. 2019. p. 79–88. DOI: https://doi.org/10.1007/978-3-319-93587-4_9.

3. Larshin, V. & Lishchenko, N. “Research Methodology for Grinding Systems”. *Russian Engineering Research.* 2018; Vol. 38 Issue 9: 712–713. DOI: https://doi.org/10.3103/S1068798X1809024.

4. Yakimov, A. V. “Kachestvo izgotovleniya zubchatykh koles”. [The Quality of Manufacturing Gears] (in Russian). *Publ. Mashinostroyeniye.* Moscow: Russian Federation. 1979. 191 p.

5. Evseyev, D. G. (1975). “Formirovaniye svoystv poverkhnostnykh sloyev pri abrazivnoy obrabotke”. [Formation of the Properties of Surface Layers in Abrasive Machining] (in Russian). *Izd-vo Saratov. un-ta.* Saratov: Russian Federation. 128 p.

6. Sundarrajan, K. D. “Study of Grinding Burn Using Design of Experiments Approach and Advanced Kaizen Methodology”. PhD Thesis, The graduate college at the University of Nebraska Lincoln, Nebraska. 2017. 65 p.

7. Tan, J., Jun,Y. & Siwei, P. “Determination of Burn Thresholds of Precision Gears in Form Grinding Based on Complex Thermal Modelling and Barkhausen Noise Measurements”. *The International Journal of Advanced Manufacturing Technology*. 2017; Vol. 88 Issue 1-4: 789–800. DOI: https://doi.org/10.1007/ s00170-016-8815-x.

8. Jun, Y. & Ping, L. “Temperature Distributions in Form Grinding of Involute Gears”. *The International Journal of Advanced Manufacturing Technology*. 2017; Vol.88 Issue 9-12: 2609–2620. DOI: https://doi.org/10.1007/s00170-016-8971-z.

9. Jermolajev, S., Epp, J., Heinzel, C. & Brinksmeier, E. “Material Modifications Caused by Thermal and Mechanical Load during Grinding”. *3rd CIRP conference on surface integrity (CIRP CSI). Procedia CIRP* 45. 2016. p. 43–46. DOI: https://doi.org/10.1016/j.procir.2016.02.159.

10. Jermolajev, S., Brinksmeier, E. & Heinzel, C. “Surface Layer Modification Charts for Gear Grinding”. *CIRP Annals – Manufacturing Technology*. 2018; 67(1): 333–336. DOI: https://doi.org/10.1016/ j.cirp.2018.04.071.

11. Heinzel, C., Sölter, J., Jermolajev, S., Kolkwitz, B. & Brinksmeier, E. “A Versatile Method to Determine Thermal Limits in Grinding”. *2nd CIRP Conference on Surface Integrity (CSI) Procedia CIRP 13*. 2014. p. 131–136. DOI: https://doi.org/10.1016/j.procir.2014.04.023.

12. Malkin, S. & Guo, C. “Thermal Analysis of Grinding”. *CIRP Annals Manufacturing Technology*. 2007; Vol.56, Issue 2: 760–782. DOI: https://doi.org/10.1016/j.cirp.2007.10.005.

13. Karpuschewski, B., Bleicher, O. & Beutner, M. “Surface Integrity Inspection on Gears Using Barkhausen Noise Analysis”. *1st CIRP Conference on Surface Integrity (CSI) Procedia Engineering* 19. 2011. p. 162–171. DOI: https://doi.org/10.1016/j.proeng.2011.11.096.

14. Vrkoslavová, L., Louda, P. & Malec, J. “Analysis of Surface Integrity of Grinded Gears Using Barkhausen Noise Analysis and X-Ray Diffraction”. *40th Annual Review of Progress in Quantitative Nondestructive Evaluation APP Conf*. Proc. 1581. 2014. p. 1280–1281. DOI: https://doi.org/10.1063/1.4864968.

15. Crow, J. R. & Michael A. “Pershing Standard Samples for Grinder Burn Etch Testing”, *Gear Technology*. 2018. p. 54–56.

16. Mazuru, S., Casian, M. & Scaticailov, S. “The Processing Accuracy of the Gear”. *MATEC Web of Conferences* 112, 01026. 2017. p. 1–6. DOI: https://doi.org/10.1051/matecconf/201711201026.

17. Wojtas, A. S., Suominen, L., Shaw, B. A. & Evans, J. T. “Detection of Thermal Damage in Steel Components after Grinding Using the Magnetic Barkhausen Noise Method”, https://www.ndt.net/article/ecndt98/aero/041/041.htm. 1998.

18. Zaborowski, T. & Ochenduszko, R. “Grinding Burns in the Technological Surface of the Gear Teeth of the Cylindrical Gears”. *MECHANIK NR.* 10. DOI: https:// doi.org/10.17814/mechanik.2017.10.135.

19. Blake, G., Margetts M. & Silverthorne, W. “Gear Failure Analysis Involving Grinding Burn”. *Gear technology*. January/February 2009. p. 62–66.

20. “No Compromising on Quality at Allison Transmission”. *Technology*. July 2014. p. 22–24.

21. Gorgels, C., Klocke, F. & Schröder, T. “Influence of Grinding Burn on Pitting Capacity”. *Gear Technology*. August 2008. p. 58–63.

22. Korn, D. Applying Inductive Technology to Detect Grinding Burn. Available at: https://www.mmsonline. com/articles/applying-inductive-technology-to-detect-grinding-burn.

23. Klocke, F. & Schlattmeier, H. “Surface Damage Caused by Gear Profile Grinding and its Effects on Flank Load Carrying Capacity”. *Gear technology.* September/October 2004. p. 44–53.

24. André de Lima, Gâmbaro, L. S., Junior, M. V. & Baptista, E. B. “The Use of Cylindrical Grinding to Produce a Martensitic Structure on the Surface of 4340 Steel”. DOI: https://doi.org/10.1590/S1678-58782011000100005.

25. Golgels, C., Schlattmeier, H. & Klocke, H. “Optimization of the Gear Profile Grinding Process Utilizing an Analogy Process”, *Gear technology*. November/December 2006. p. 34–40.

26. Lishchenko, N. V. & Larshin, V. P “Profile Gear Grinding Temperature Determination”. *In: 4th International Conference on Industrial Engineering*. ICIE Lecture Notes in Mechanical Engineering. *Publ. Springer*. 2019. p. 1723–1730. DOI: https://doi.org/10.1007/978-3-319-95630-5_185.

27. Deivanathan, R. & Vijayaraghavan, L. “Theoretical Analysis of Thermal Profile and Heat Transfer in Grinding”. *International Journal of Mechanical and Materials Engineering* (IJMME). 2013; Vol.8 Issue1: 21–31.

28. Yadav, Mr. R. K. “Analysis of Grinding Process by the Use of Finite Element Methods”. *ELK Asia Pacific Journal of Manufacturing Science and Engineering*. 2014; Vol.1 Issue1: 35–42.

29. Foeckerer, T., Zaeh, M. & Zhang, O. „A Three-Dimensional Analytical Model to Predict the Thermo-Metallurgical Effects within the Surface Layer during Grinding and Grind-Hardening”. *International Journal of Heat and Mass Transfer*. 2013; Vol.56 Issue 1-2: 223–237. DOI: https://doi.org/10.1016/j.ijheatmasstransfer.2012.09.029.

30. González-Santander, J. L “Maximum Temperature in Dry Surface Grinding for High Peclet Number and Arbitrary Heat Flux Profile”. *Hindawi Publishing Corporation Mathematical Problems in Engineering*. Article ID 8470493.2016; Vol.2016: 1–9. DOI: http://doi.org/10.1155/2016/8470493.

31. Guo, C. & Malkin, S. “Analysis of Transient Temperatures in Grinding”. *Journal of Engineering for Industry*. 1995; Vol.117 Issue 4: 571–577. DOI: https://doi.org/doi:10.1115/1.2803535.

32. Beizhi, L., Dahu, Z., Zhenxin, Z., Qiang, Z. & Yichu, Y. “Recearch on Workpiece Surface Temperature and Surface Quality in High-Speed Cylindrical Grinding and its Inspiration”. *Advanced Materials Research.* 2011; 325: 19–27. DOI: https://doi.org/10.4028/www.scientific.net/AMR.325.19.

33. Li Hao N. & Axinte, D. ”On a Stochastically Grain-Discretised Model for 2D/3D Temperature Mapping Prediction in Grinding”, *International Journal of Machine tools and manufacture 116.* 2017.01.004. p. 1–27. DOI: https://doi.org/10.1016/j.ijmachtools.

34. Tadeu, A. & Simoes, N.”Three-Dimensional Fundamental Solutions for Transient Heat Transfer by Conduction in an Unbounded Medium, Half-Space, Slab and Layered Media”, *Engineering Analysis with Boundary Elements.* 2006; 30(5): 338–349. DOI: https://doi.org/ 10.1016/j.enganabound.2006.01.011.

35.Chen, Xun & Öpöz, T “Effect of Different Parameters on Grinding Efficiency and its Monitoring by Acoustic Emission”, *Production & Manufacturing Research. An Open Access Journal*. 2016. 4(1). 190–208. DOI: https://doi.org/10.1080/21693277.2016.1255159.

ISSN 2617-4316 (Print)
ISSN 2663-7723 (Online)

36. Linke, B., Duscha, M., Vu, A. T. & Klocke F. “FEM-Based Simulation of Temperature in Speed Stroke Grinding with 3D Transient Moving Heat Sources”. *Advanced Materials Research.* 2011; Vol.223: 733–742. DOI: https://doi.org/10.4028/ www.scientific.net/AMR.223.73.

37. Patil Prashant & Patil Chandrakant. “FEM Simulation and Analysis of Temperature Field of Environmental Friendly MQL Grinding”. *Proceedings of the international conference on communication and signal processing 2016.* p. 182–186.

38. Sharma, C., Ghosh, S. & Talukdar, P. “Finite Element Analysis of Workpiece Temperature during Surface Grinding of Inconel 718 Alloy”. *In: 5th international & 26th all India manufacturing technology, design and research conference. IIT Guwahati.* Assam: India. 2014. p. 420-1 – 420-6.

39. Rena, X. & Hu, H. “Analysis on the Temperature Field of Gear Form Grinding”, *Applied Mechanics and Materials.* 2014: 633-634: 809–812. DOI: https://doi.org/10.4028 /www.scientific.net/AMM.633-634.809.

40. Mahdi, M. & Liangchi, Z. “The Finite Element Thermal Analysis of Grinding Processes by ADINA”. *Computers & Structures.* 1995; Vol.56 Issue 2-3: 313–320. DOI: https://doi.org/10.1016/0045-7949(95)00024-B.

41. Zhang, L. “Numerical Analysis and Experimental Investigation of Energy Partition and Heat Transfer in Grinding”. In: M. SalimNewazKazi (Eds.). *Heat Transfer Phenomena and Applications. Sense Publishers*, Rotterdam, the Netherlands. 2012. p. 79–98. DOI: https://doi.org/10.5772/52999.

42. Larshin, V. P. “Tekhnologiya mnogonitochnogo rezboshlifovaniya pretsizionnykh khodovykh vintov” [Multi-Thread Grinding Technology for Precision Ball Screws] (in Russian).Trudy Odes. politekhn. un-ta. Odessa: Ukraine. 1999; 2(8): 87–91

43. Lishchenko, N. “Profile Gear Grinding Temperature Determination”, *Transactions of Kremenchuk Mykhailo Ostrohradskyi National University*. 2018; 1(108): 100–108.

44. Carslaw, H. S. & Jaeger, J. S. “Conduction of Heat in Solids”. *Oxford University Press;* 2-ed. Great Britain: Oxford. 1959.

45. Larshin, V. P, Kovalchuk, E. N. & Yakimov, A. V. “Primenenie resheniy teplofizicheskikh zadach k raschetu temperatury i glubiny defektnogo sloya pri shlifovanii”, [Application of Solutions of Thermo-Physical Problems to the Calculation of the Temperature and Depth of the Defective Layer during Grinding] (in Russian). Interuniversity collection of scientific works, Perm. 1986. p. 9–16

46. Sipaylov, V. A. “Teplovye protsessy pri shlifovanii i upravlenie kachestvom poverkhnosti”. [Thermal Processes during Grinding and Surface Quality Control] (in Russian). *Publ. Mashinostroenie.* Moscow: Russian Federation. 1978.

Conflicts of Interest: the authors declare no conflict of interest

Received 12.09.2019
Received after revision 09.11. 2019
Accepted 02.12.2019

DOI: https://doi.org/ 10.15276/aait.02.2019.5
УДК 621.923.1:621.833

ПОРІВНЯННЯ ВИМИРЮВАНИХ ПАРАМЕТРІВ ЯКОСТІ ПОВЕРХНЕВОГО ШАРУ З РЕЗУЛЬТАТАМИ МОДЕЛЮВАННЯ

Наталя Володимирівна Ліщенко[1)]
ORCID: 0000-0002-4110-1321, odeslnv@gmail.com
Василь Петрович Ларшин[2)]
ORCID: 0000-0001-7536-3859, vasilylarshin@gmail.com
[1)] Одеська національна академія харчових технологій, вул. Канатна, 112. Одеса, 65039, Україна
[2)] Одеський національний політехнічний університет,пр. Шевченка, 1. Одеса, 65044, Україна

АНОТАЦІЯ

Температура шліфування є одним з факторів, що обмежує продуктивність профільного шліфування зубчастого колеса. Існує два основних методи визначення температури шліфування: аналітичний метод за допомогою аналітичних моделей і імітаційний, заснований як на аналітичних, так і на геометричних моделях. У статті на першому етапі досліджують температурне поле профільного зубошліфування за допомогою методу кінцевих елементів (FEM) як приклад інформаційної технології, що допомагає прогнозувати фізичні параметри якості поверхневого шару. Отримані результати порівнюють з аналогічними розрахунками для аналітичних моделей, і знаходять ділянки поверхні зуба для визначення температури відповідно до аналітичних моделей. На другому етапі проведено серія експериментальних досліджень на верстаті з ЧПК Höfler Rapid 1250 при шліфуванні реального зубчастого колеса при послідовному збільшенні глибини профільного шліфування. З обробленого зубчастого колеса вирізали спеціальні зразки на електроерозійному верстаті мод. MV 2400S ADVANCE Type 2 (MITSUBISHI ELECTRIC Company) для додаткового дослідження цих зразків. Експериментальне дослідження якості поверхневого шару зубів і структурно-фазового стану поверхневого шару проведено з використанням сучасного вимірювального встаткування й приладів,

наприклад, мікроскопа Altami MET-5. Встановлено, що за інших рівних умов більш висока температура шліфування має місце у верхній частині зуба при шліфуванні. Виявлено ділянки профілю зуба, по яких можна розрахувати температуру шліфування за відомими аналітичними залежностями. Встановлено, що при збільшенні параметрів, що характеризують інтенсивність шліфування і обсяг знімання матеріалу на одиницю ширини шліфувального круга, шліфувальний припік виникає і його товщина збільшується. Встановлена закономірність зміни товщини припіку по висоті зуба, що дозволяє оцінити вірогідність відповідних теоретичних досліджень за інформаційними моделями.

Ключові слова: профільне шліфування зубчастого колеса, шліфувальний припік, якість поверхневого шару, температура шліфування; FEM моделювання

DOI: https://doi.org/ 10.15276/aait.02.2019.5
УДК 621.923.1:621.833

СРАВНЕНИЕ ИЗМЕРЕННЫХ ПАРАМЕТРОВ КАЧЕСТВА ПОВЕРХНОСТНОГО СЛОЯ С РЕЗУЛЬТАТАМИ МОДЕЛИРОВАНИЯ

Наталья Владимировна Лищенко[1)]
ORCID: 0000-0002-4110-1321, odeslnv@gmail.com
Василий Петрович Ларшин[2)]
ORCID: 0000-0001-7536-3859, vasilylarshin@gmail.com
[1)] Одесская национальная академия пищевых технологий, ул. Канатная, 112. Одесса, 65039, Украина
[2)] Одесский национальный политехнический университет, пр. Шевченко, 1. Одесса, 65044, Украина

АННОТАЦИЯ

Температура шлифования является одним из факторов, ограничивающих производительность профильного шлифования зубчатого колеса. Существует два основных метода определения температуры шлифования: аналитический метод с помощью аналитических моделей, и имитационный, основанный как на аналитических, так и на геометрических моделях. В статье на первом этапе исследуется температурное поле профильного зубошлифования с помощью метода конечных элементов (FEM) в качестве примера информационной технологии, которая помогает прогнозировать физические параметры качества поверхностного слоя. Полученные результаты сравниваются с аналогичными расчётами для аналитических моделей, и определяются участки поверхности зуба для определения температуры в соответствии с аналитическими моделями. На втором этапе проводится серия экспериментальных исследований на станке с ЧПУ Höfler Rapid 1250 при зубошлифовании реального зубчатого колеса при последовательном увеличении глубины профильного шлифования. Из обработанного шлифованием зубчатого колеса вырезали специальные образцы на электроэрозионном станке мод. MV 2400S ADVANCE Type 2 (MITSUBISHI ELECTRIC Company) для дополнительного исследования этих образцов. Экспериментальное исследование качества поверхностного слоя зубьев и структурно-фазового состояния поверхностного слоя проводилось с использованием современного измерительного оборудования и приборов, например, микроскопа Altami MET-5. Установлено, что при прочих равных условиях более высокая температура шлифования имеет место в верхней части шлифованного зуба. Выявлены участки профиля зуба, по которым можно рассчитать температуру шлифования по известным аналитическим зависимостям. Установлено, что при увеличении параметров, характеризующих интенсивность шлифования и объем съема материала на единицу ширины шлифовального круга, шлифовальный прижог возникает и его толщина увеличивается. Установлена закономерность изменения толщины прижога по высоте зуба, что позволяет оценить достоверность соответствующих теоретических исследований по информационным моделям.

Ключевые слова: профильное шлифование зубчатого колеса, шлифовочный прижог, качество поверхностного слоя, температура шлифования, FEM моделирование

ABOUT THE AUTHORS

Natalia V. Lishchenko – PhD (Eng) (2006), Dr. Sci. (Eng) (2018), Dean of Faculty of Computer Science and Automation, Professor of the Department of Electromechanics, Mechatronics and Engineering Graphics. Odessa National Academy of Food Technologies, 112, Kanatna Str. Odesa, 65039, Ukraine
ORCID: https://orcid.org/0000-0002-4110-1321; odeslnv@gmail.com.
Research field: Information Support of Technological Processes

Наталя Володимирівна Ліщенко – кандидат технічних наук (2006), доктор технічних наук (2018), декан факультету Комп'ютерних систем та автоматизації, професор кафедри Електромеханіки, мехатроніки та інженерної графіки. Одеська національна академія харчових технологій, вул. Канатна, 112. Одеса, 65039,Україна

Vasily Petrovich Larshin – PhD (Eng) (1980), Dr. Sci. (Eng) (1995), Academician of the Ukrainian Academy of Economic Cybernetics (2020). Professor of Department of Mechanical Engineering Technology. Odessa National Polytechnic University, 1, Shevchenko Ave. Odesa, 65044, Ukraine
ORCID: https://orcid.org/0000-0001-7536-3859; vasilylarshin@gmail.com.
***Research field*:** Production and Technological Processes Information Ensuring

Василь Петрович Ларшин – кандидат технічних наук (1980), доктор технічних наук (1995), академік Української академії економічної кібернетики (2020), професор кафедри Технології машинобудування. Одеський національний політехнічний університет, пр. Шевченка, 1. Одеса, 65044, Україна